INDERSCIENCE PUBLISHERS
Linking academia, business and industry through research

International Journal of Data Mining and Bioinformatics

ISSN online: 1748-5681 - ISSN print: 1748-5673
https://www.inderscience.com/ijdmb

Core genes and pathways underlying ferroptosis in chondrosarcoma pathogenesis: through bioinformatics analysis

Zhiqiang Ye, Zhaoyuan Wang, Zhuo Zhao, Yongxu Zhang, Bowen Zheng, Lianbo Yang, Jinghang Lu, Haidong Liang

DOI: 10.1504/IJDMB.2026.10079732

Article History:

Received:	22 August 2025
Last revised:	12 December 2025
Accepted:	11 March 2026
Published online:	28 August 2026

Core genes and pathways underlying ferroptosis in chondrosarcoma pathogenesis: through bioinformatics analysis

Zhiqiang Ye

Department of Bone and Soft Tissue
Repair and Reconstructive Surgery,
The Second Hospital of Dalian Medical University,
Dalian Liaoning 116000, China
Email: 18782835120@163.com

Zhaoyuan Wang

Department of Aesthetic Plastic Surgery and Laser Medicine,
Beijing Anzhen Hospital,
Capital Medical University,
Beijing 100029, China
Email: shuying9313@163.com

Zhuo Zhao, Yongxu Zhang, Bowen Zheng, Lianbo Yang, Jinghang Lu and Haidong Liang*

Department of Bone and Soft Tissue
Repair and Reconstructive Surgery,
The Second Hospital of Dalian Medical University,
Dalian Liaoning 116000, China
Email: zhaozhuo0331@163.com
Email: z2938769115@163.com
Email: 18540051905@163.com
Email: yangliandoctor@163.com
Email: 15566610125@163.com
Email: lianghaidong751028@outlook.com
*Corresponding author

Abstract: Chondrosarcoma (CS) often resists standard radiotherapy and chemotherapy. Our study explores ferroptosis as a novel tactic to counter this resistance, investigating molecular mechanisms in CS and identifying core genes impacting patient survival rates. The database was screened for 2,821 DEGs and 471 ferroptosis-related genes. Further analysis by Gene-miRNA and PPI networks identified nine core genes (*IL6*, *TP53*, *MAPK1*, *CAV1*, *GJA1*, *SMAD7*, *TXNIP*, MAP3K5, and *DUSP1*) related to ferroptosis in CS. Lower expression of *IL6*, *TP53*, *MAPK1*, and *SMAD7*, alongside higher expression of *CAV1*, *GJA1*, *TXNIP*, *MAP3K5*, and *DUSP1* were noted in CS tissues. Survival analysis demonstrated higher survival rates in CS patients with low *GJA1* and

high *IL6* expression. In conclusion, *GJA1* and *IL6* may play pivotal roles in the regulation of ferroptosis in CS, and are tightly associated with the prognosis of CS patients.

Keywords: ferroptosis; chondrosarcoma; *GJA1*; *IL6*.

Reference to this paper should be made as follows: Ye, Z., Wang, Z., Zhao, Z., Zhang, Y., Zheng, B., Yang, L., Lu, J. and Liang, H. (2026) 'Core genes and pathways underlying ferroptosis in chondrosarcoma pathogenesis: through bioinformatics analysis', *Int. J. Data Mining and Bioinformatics*, Vol. 30, No. 8, pp.1–23.

Biographical notes: Zhiqiang Ye is a Master degree candidate in orthopaedics with a solid foundation in both the clinical theory and practice of orthopaedics.

Zhaoyuan Wang is a Master degree candidate in plastic surgery with a solid foundation in both the clinical theory and practice of plastic surgery.

Zhuo Zhao is an attending physician with eight years of clinical experience. He serves as a committee member of the Wound Repair Branch of the Chinese Medical Promotion Association and is proficient in the clinical diagnosis and surgical management of common orthopaedic conditions.

Yongxu Zhang is a Master degree candidate in orthopaedics, possessing both systematic theoretical knowledge and standardised clinical skills in the field of orthopaedics.

Bowen Zheng is a Master degree candidate in orthopedics, specialising in the management of complex cases through a multidisciplinary collaborative approach and emphasising personalised treatment.

Lianbo Yang, a master degree candidate in orthopedics, skilled at deeply integrating cutting-edge research findings with clinical practice, and has contributed to the publication of multiple SCI-indexed papers.

Jinghang Lu is a Master degree candidate in orthopaedics, possessing comprehensive management capabilities spanning the entire treatment cycle – from disease diagnosis and surgical procedures to postoperative rehabilitation.

Haidong Liang is a Chief Physician and Doctoral Advisor who holds several academic positions, including young member of the Microsurgery Branch of the Chinese Medical Association and Vice Chair of the Microsurgery Branch of the Liaoning Medical Association.

1 Introduction

Chondrosarcoma (CS) is a primary bone malignancy originating from chondrocytes with an estimated incidence of 0.5 per 100,000 patient-years (Pennington et al., 2021) and is the second most common primary bone malignancy (Chow, 2018). CS grows slowly and commonly affect adults over 30 years old. CS frequently occurs at the ilium and the proximal end of long bones, mainly manifesting as pain and swelling. Depending on the degree of pathological differentiation, CS can be classified into grade 1–3, with more

than 90% of cases being grade 1–2, 5%–10% of cases as grade 3 (Weinschenk et al., 2021). Grade 3 lesions are characterised by a poor prognosis, high metastatic potential, and the highest local recurrence rate. The occurrence of recurrence is indicative of a poor prognosis. Additionally, Grade 3 lesions have a lung metastasis rate exceeding 50% and a ten-year survival rate below 30% (Weinschenk et al., 2021). The five-year survival rates for patients with low-grade, high-grade, and dedifferentiated CS were reported as 83%, 53%, and 7%–24% respectively (Miwa et al., 2022). The main treatment for CS is surgery, as CS is generally not responsive to radiotherapy and chemotherapy (Weinschenk et al., 2021). However, recurrence within five years after surgery is common, and the prognosis is often poor, with a significant increased risk of metastasis and overall mortality (Thorkildsen et al., 2021). The number of patients with clinically metastatic or surgically unresectable advanced CS is small, and their distribution is not concentrated, resulting in limited related therapeutic options and suboptimal outcomes. Furthermore, there is a lack of clinical trial studies focusing on CS. The unclear understanding of the pathogenesis of CS further complicates the design of effective treatment plans for patients. Therefore, there is an urgent need to explore the potential mechanisms underlying CS and develop strategies to improve the survival rate of CS patients in clinical practice.

Previous studies have demonstrated the involvement of programmed cell death in the occurrence of CS. For instance, Programmed Cell Death 5 (*PDCD5*) is a novel apoptosis-related gene and Chen et al. (2010) have found that *PDCD5*is downregulated in CS and might be an independent prognostic factor for overall survival of CS patients. Ferroptosis is a novel iron-dependent, non-apoptotic regulated form of cell death (Luo et al., 2021), referring to lipid peroxidation, iron accumulation, reactive oxygen species (ROS) production, and glutathione deprivation (Qiu et al., 2022). It is closely related to various physiological and pathological processes, including normal development, ischemic damage, degenerative diseases, immune system activity, and importantly, tumour biology (Stockwell et al., 2020, 2017). Ferroptosis has great therapeutic potential in osteosarcoma (Liu et al., 2022) and effective in a variety of tumours (Chen et al., 2021). In osteosarcoma, Liu et al. first uncovered iron-dependent and non-apoptotic ferroptosis-like cell death in osteosarcoma cell line D-27, which can induce ferroptosis by inhibiting signal transducer and activator of transcription 3 (STAT3)/nuclear factor erythroid 2-related factor 2 (Nrf2)/glutathione peroxidase 4 (GPX4) signal (Liu and Wang, 2019). Emerging evidence has convincingly demonstrated the close association between ferroptosis and the development of osteosarcoma (Jiang et al., 2023; Ma et al., 2024). However, the association between ferroptosis and CS has been relatively understudied, and the key factors involved in the ferroptosis mechanism of CS remain unclear, particularly those influencing the survival rate of CS patients.

At present, the understanding of how ferroptosis contributes to the pathogenesis and prognosis of CS is not clear, and there is also a lack of relevant bioinformatics research, emphasising the need for further research to elucidate the role of ferroptosis in CS and its impact on patient outcomes. In this study, we performed a comprehensive bioinformatics analysis to investigate the molecular pathogenesis of ferroptosis in CS and identify potential core genes that may impact the survival rate of CS patients. Our research results will help to understand the ferroptosis in CS, and provide new ideas and targets for the clinical treatment of CS.

2 Material and methods

2.1 Screen of differentially expressed genes (DEGs)

The transcriptome expression profile data (GSE48418 and GSE30835) of CS was downloaded from Genome Expression Omnibus (GEO; https://www.ncbi.nlm.nih.gov/geo/). The limma::normalizeBetweenArrays function in R was used to perform quantile normalisation on the data. If the maximum value in the normalised expression matrix was exceeded 100, then a $\log_2(x + 1)$ transformation was applied to the data to make the distribution of expression values closer to a normal distribution and to effectively compress the extremely high values. Subsequently, the corresponding annotation file of the platform was downloaded and the probe ID along with the corresponding gene Symbol was extracted. When multiple probes were mapped to the same gene, the arithmetic mean of the expression levels of these probes was calculated as the final expression value of the gene. In this study, GSE48418 dataset was used as the training set, and GSE30835 dataset was employed as the validation set to confirm the expression level of the identified core genes. A schematic workflow diagram of this study is shown in Figure 1. The DEGs were screened using Limma package (Ritchie et al., 2015). The screening conditions were set as p-value < 0.05 and |logFC| > 1 (Song et al., 2024; Liu and Liu, 2025).

Figure 1 A schematic workflow diagram of this study

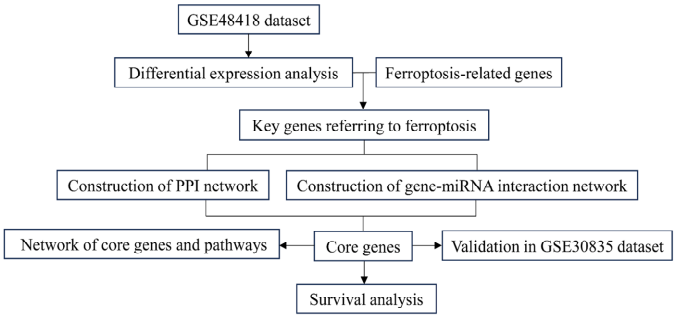

2.2 Search of key genes referring to ferroptosis in CS

The genes associated with ferroptosis, including Driver, Suppressor, Marker, and Unclassified genes, were queried in the FerrDb database (http://www.zhounan.org/ferrdb/current/). Merge the results and remove duplicate genes. Subsequently, the DEGs and the key genes were compared using VennDiagram to identify the overlapping genes (Chen and Boutros, 2011).

2.3 Construction of Gene-miRNA interaction network

The overlapping genes obtained in the previous step was input into the 'miRNA-mRNA' interaction module of ENCORI database (starBase Version 2.0 platform, https://starbase.sysu.edu.cn/) with the screening condition of dual evidence of 'Clip-Seq experimental support + miRanda prediction', and the confidence threshold was

set to miRanda score ≥ 140 and energy ≤ –20 kcal/mol. Then the Gene-miRNA interaction pairs were wrapped using ggraph (Version 2.1.0) and igraph (Version 1.4.1) in R language.

2.4 Biological function enrichment analysis

Gene ontology (GO) enrichment analysis and Kyoto Encyclopaedia of Genes and Genomes (KEGG) pathway analysis were performed on the intersection genes using the clusterProfiler package (Yu et al., 2012) in R language (Version 4.2). The analysis included screening conditions with a defined threshold of p-value < 0.05.

2.5 Construction of protein-protein interaction (PPI) network

The interaction relationships of the overlapping genes were predicted using STRING database (Version 12.0) (Szklarczyk et al., 2021) and the screening conditions were as follows score_cutoff > 0.4 and size_cutoff < 10. Interaction relationships of the PPI network were visualised by Cytoscape software (Version 3.9.0). The hub-genes in the PPI network were screened using the CytoHubba plugin and identified based on the Degree, MCC, EPC and MNC algorithms. Then the top 20 genes obtained from degree, MCC, EPC and MNC algorithms were intersected, and the common genes were considered as the hub genes.

2.6 Screening of core genes associated with ferroptosis in CS

The hub-genes obtained from the Gene-miRNA network were intersected with those got from the PPI network by VennDiagram. The newly obtained intersection genes represent core genes associated with ferroptosis in CS, which could be utilised for further analysis.

2.7 Building the network of core genes and pathways

The top 30 GO terms and pathways associated with the core genes in the above GO and KEGG pathway enrichment analysis were selected and visualised using Cytoscape software (Version 3.9.0) to examine their relationship pairs.

2.8 Core genes expression in patients with CS

A t-test was performed to compare the expression levels of the core genes between CS and normal tissue based on the transcriptome expression profile data (GSE48418) of CS. Also, the expression levels of the core genes between CS and normal tissue were confirmed in GSE30835 dataset.

2.9 Survival Analysis of CS patients: impact of core genes

The core genes were analysed using the GEPIA platform (http://gepia.cancer-pku.cn/) to investigate their impact on the survival of patients based on TCGA-SARC cohort. The survival time of patients with high-expression and low-expression core genes was compared using the log-rank test. Genes with a P-value less than 0.05 were considered as the genes of interest.

3 Results

3.1 Screening of key genes associated with ferroptosis in CS

A total of 2,821 DEGs were identified in CS using the Limma package [Figure 2(a)]. The top 50 DEGs were visualised in a heat map [Figure 2(b)]. Subsequently, 471 ferroptosis-related genes were selected based on the FerrDb database. Through intersection analysis, 70 key genes associated with ferroptosis in CS were identified [Figure 2(c), Table S1].

Figure 2 Screening for ferroptosis-related genes acting in chondrosarcoma (CS), (a) volcano plot of DEGs in the transcriptome expression profile data (GSE48418) of CS (b) heat map of the top 50 DEGs according to |logFC| value> 1 (c) Venn diagram of the intersection genes of CS and ferroptosis (see online version for colours)

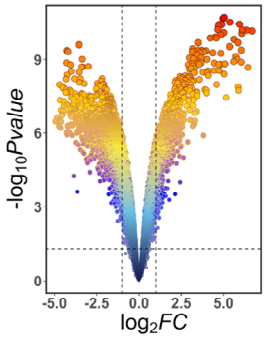

(a)

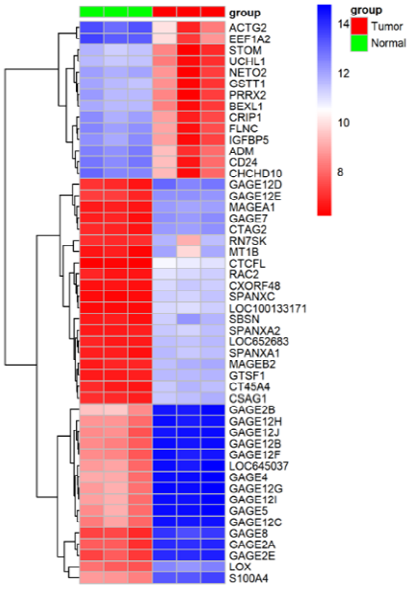

(b)

Figure 2 Screening for ferroptosis-related genes acting in chondrosarcoma (CS), (a) volcano plot of DEGs in the transcriptome expression profile data (GSE48418) of CS (b) heat map of the top 50 DEGs according to |logFC| value> 1 (c) Venn diagram of the intersection genes of CS and ferroptosis (continued) (see online version for colours)

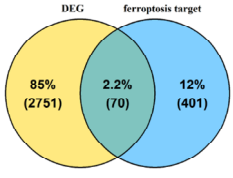

(c)

3.2 Obtention of hub-genes from Gene-miRNA interaction network

Based on the ENCORI database, totally 1,452 gene-miRNA interaction pairs were obtained [Figure 3(a)] and the top 20 genes with larger degree in R were extracted as hub-genes. GO and KEGG enrichment analyses were conducted on the 70 intersection genes to gain insights into their functional roles and involvement in signalling pathways. A total of 603 enriched GO terms and 22 significant KEGG signalling pathways were identified. The top five BP terms such as cellular response to external stimulus and cellular response to extracellular stimulus, CC terms such as autolysosome and ficolin-1-rich granule, and MF terms such as protein ADP-ribosylase activity and NAD^+ |ADP-ribosyltransferase activity, were shown in Figure 3(b) and Table 1. The top 15 enrichment pathways such as toll-like receptor (TLR) signalling pathway and MAPK signalling pathway were shown in Figure 3(c) and Table 2 according to the p-value.

Figure 3 The gene-miRNA interaction network and GO/KEGG enrichment analysis, (a) the gene-miRNA interaction network (the larger the size, the higher the degree) (b) the top 5 BP, CC, and MF terms in GO enrichment (c) the top 15 pathways in KEGG enrichment (see online version for colours)

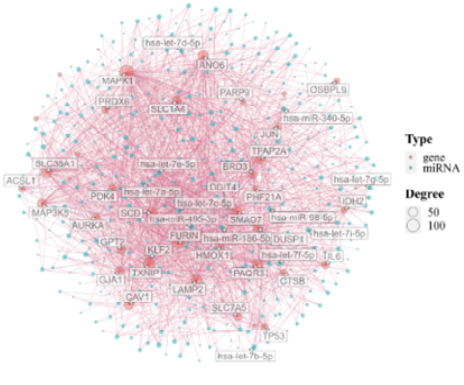

(a) (b)

Figure 3 The gene-miRNA interaction network and GO/KEGG enrichment analysis, (a) the gene-miRNA interaction network (the larger the size, the higher the degree) (b) the top 5 BP, CC, and MF terms in GO enrichment (c) the top 15 pathways in KEGG enrichment (continued) (see online version for colours)

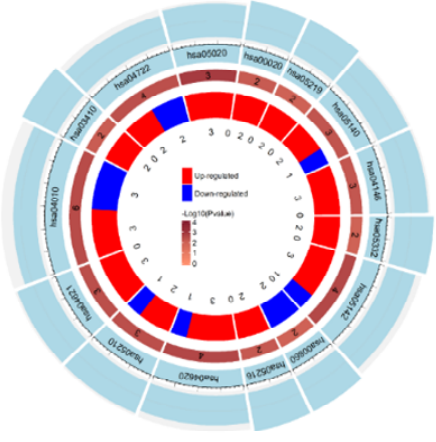

(c)

Table 1 The top five enriched terms in BP, CC, and MF categories

Ontology	*ID*	*Description*	*P-value*
BP	GO:0071496	Cellular response to external stimulus	1.12E-11
BP	GO:0031669	Cellular response to nutrient levels	2.29E-11
BP	GO:0031668	Cellular response to extracellular stimulus	1.10E-10
BP	GO:0009267	Cellular response to starvation	3.12E-10
BP	GO:0140289	Protein mono-adp-ribosylation	4.90E-10
CC	GO:0101002	Ficolin-1-rich granule	5.25E-05
CC	GO:1904813	Ficolin-1-rich granule lumen	8.24E-05
CC	GO:0044754	Autolysosome	0.000680727
CC	GO:0034774	Secretory granule lumen	0.001031025
CC	GO:0060205	Cytoplasmic vesicle lumen	0.001081397
MF	GO:1990404	Protein ADP-ribosylase activity	2.94E-09
MF	GO:0003950	NAD+ ADP-ribosyltransferase activity	2.22E-08
MF	GO:0016763	Pentosyltransferase activity	1.16E-06
MF	GO:0044389	Ubiquitin-like protein ligase binding	0.000197801
MF	GO:0015175	Neutral amino acid transmembrane transporter activity	0.000406378

3.3 Acquisition of hub-genes from PPI network

Based on the 70 intersection genes, the PPI network was constructed [Figure 4(a)]. Then the top 20 hub-genes were selected according to the degree, MCC, MNC and EPC

algorithms and displayed in Figures 4(e)–4(e). Following intersection, 18 hub-genes were obtained using VennDiagram software [Figure 4(f)].

Table 2 The top 15 enriched pathways

ID	*Description*	*P-value*
hsa05020	Prion diseases	0.001127963
hsa04620	TLR signalling pathway	0.003010478
hsa05142	Chagas disease	0.003230078
hsa04010	MAPK signalling pathway	0.004508104
hsa04621	NOD-like receptor signalling pathway	0.005839101
hsa05210	Colorectal cancer	0.005839101
hsa04722	Neurotrophin signalling pathway	0.006409407
hsa05140	Leishmaniasis	0.009532266
hsa04146	Peroxisome	0.01100683
hsa05216	Thyroid cancer	0.012793212
hsa00020	Citrate cycle (TCA cycle)	0.014543492
hsa03410	Base excision repair	0.017351068
hsa05219	Bladder cancer	0.025849517
hsa00860	Porphyrin and chlorophyll metabolism	0.027010051
hsa05332	Graft-versus-host disease	0.028191473

Figure 4 The identification of hub genes among the 70 intersection genes, (a) PPI network of the 70 intersection genes (the deeper the colour of the bodes, the greater the connectivity) (b)–(e) the top 18 hub-genes calculated by degree, EPC, MCC, and MNC algorithms (from left to right) (f) the Venn diagram of core genes in PPI network intersection (see online version for colours)

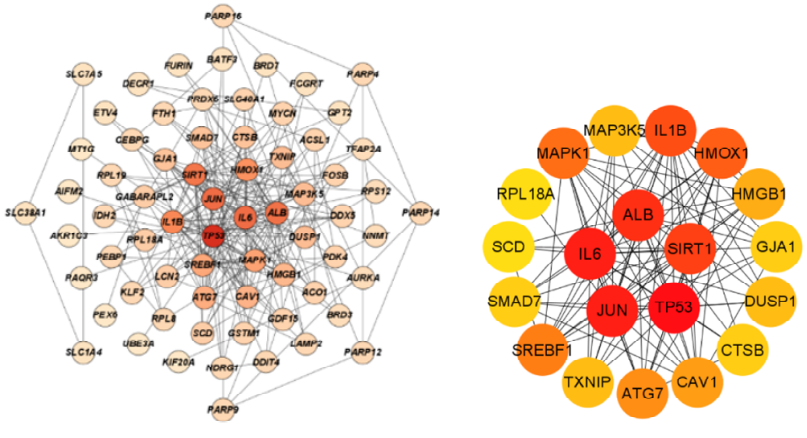

(a) (b)

Figure 4 The identification of hub genes among the 70 intersection genes, (a) PPI network of the 70 intersection genes (the deeper the colour of the bodes, the greater the connectivity) (b)–(e) the top 18 hub-genes calculated by degree, EPC, MCC, and MNC algorithms (from left to right) (f) the Venn diagram of core genes in PPI network intersection (continued) (see online version for colours)

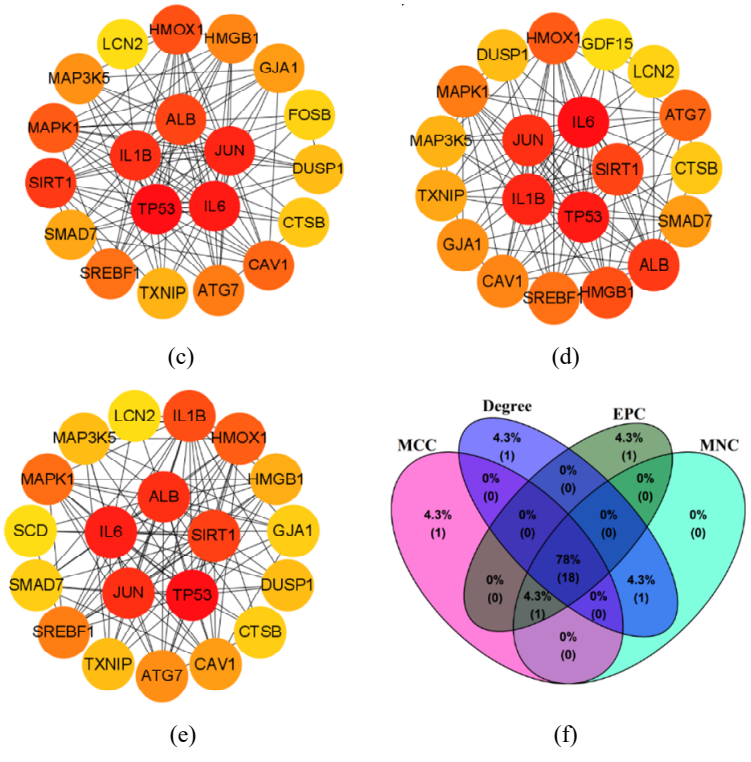

3.4 Identification of nine core genes related to ferroptosis in CS

To obtain the core genes related to ferroptosis in CS, the intersection analysis was performed between the 20 hub-genes from the gene-miRNA network and the 18 hub-genes from the PPI network. As depicted in Figure 5(a), nine core genes (*IL6*, *TP53*, *MAPK1*, *CAV1*, *GJA1*, *SMAD7*, *TXNIP*, *MAP3K5*, and *DUSP1*) associated with ferroptosis in CS were identified, indicating that these nine core genes might involve in the pathogenesis of CS. To explore the pathways associated with the core genes, a network depicting the relationship between the core genes and pathways was constructed. The top 30 pathways enriched in biological processes (BP) with a p-value < 0.05, as well as all 22 pathways enriched in the KEGG database, were selected for visualisation in Figure 5(b) (Table S2), suggesting that these nine core genes might play an important role in the development of CS via these GO-BPs and KEGG pathways.

Figure 5 Core genes related to ferroptosis in CS, (a) the Venn diagram of the intersection of the 20 hub-genes to get the core genes (b) the core genes and pathway network (see online version for colours)

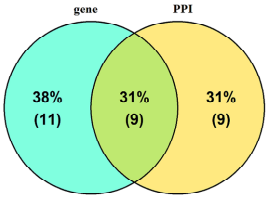

(a)

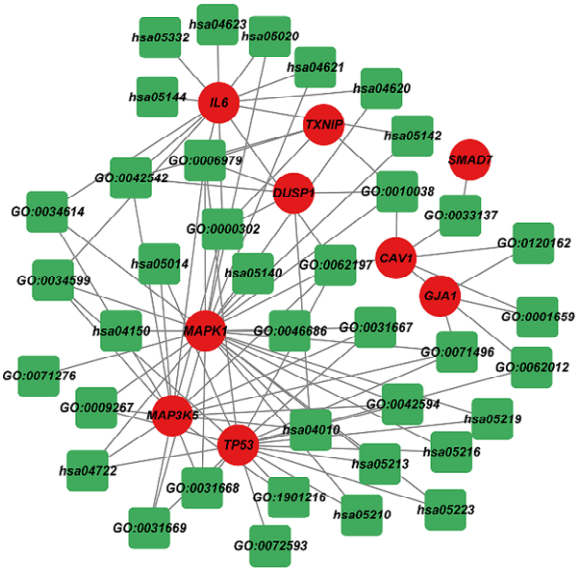

(b)

3.5 Differential expression of core genes in CS

We further evaluated the differential expression of nine core genes in normal tissue and CS. As shown in Figure 6(a), the expression of *IL6*, *TP53*, *MAPK1*, and *SMAD7* in CS was significantly lower than that in normal tissue in GSE48418 dataset, especially *IL6*, *TP53*, and *MAPK1*; while the expression of *CAV1*, *GJA1*, *TXNIP*, *MAP3K5*, and *DUSP1* was in an opposite trend ($P < 0.05$). In addition, expression levels of the nine core genes were verified in the GSE30835 dataset. As illustrated in Figure 6(b), the expression levels of *CAV1* and *GJA1* in GSE30835 dataset were consistent with those in GSE48418 dataset. Thus, it's necessary to confirm their expression stability in dataset with larger sample size.

Figure 6 Boxplot of the differential expression of nine core genes in CS compared with normal tissue, (a) in GSE48418 dataset (b) in GSE30835 dataset (see online version for colours)

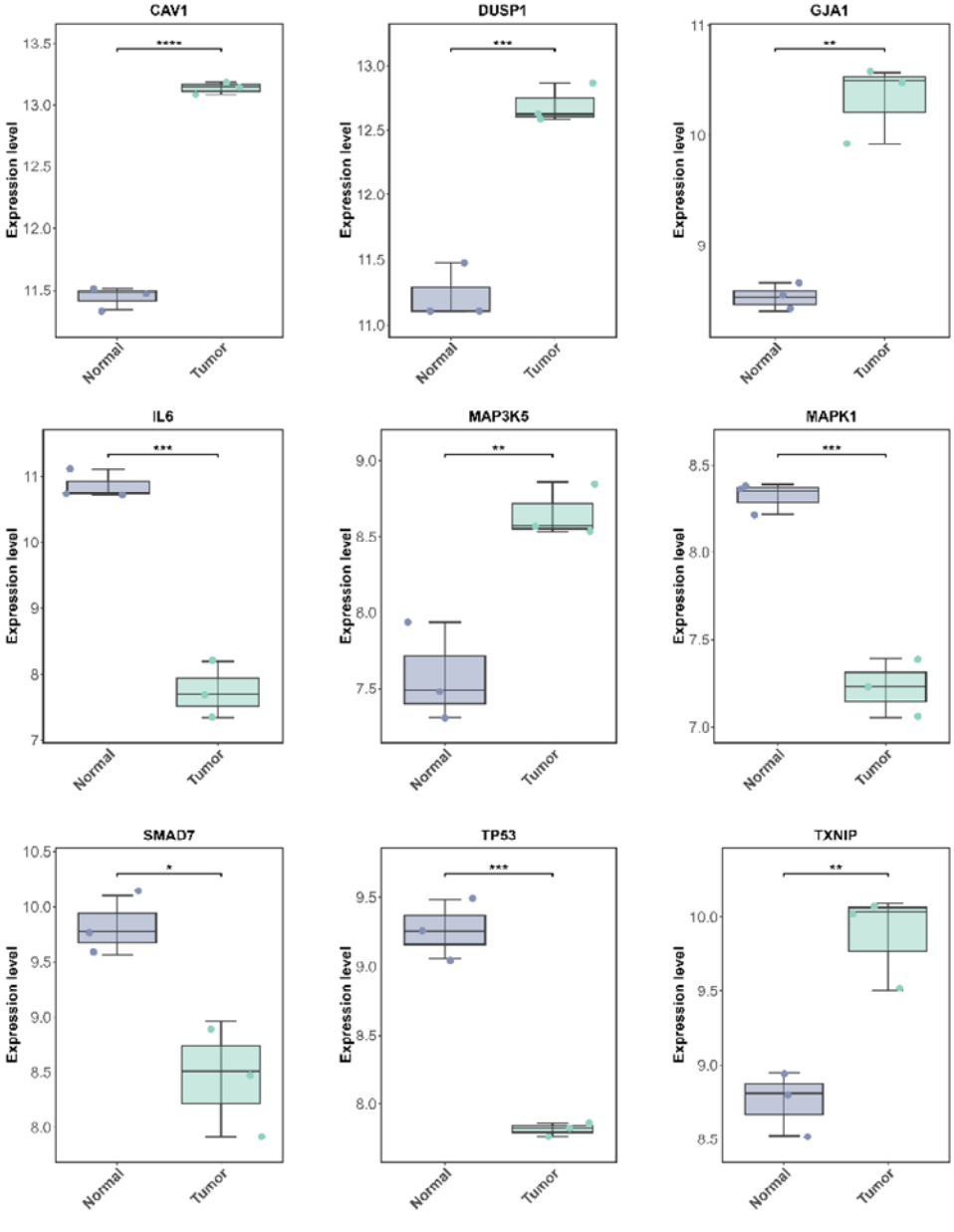

(a)

Note: *$P < 0.05$, **$P < 0.01$, ***$P < 0.001$ and ****$P < 0.0001$.

Figure 6 Boxplot of the differential expression of nine core genes in CS compared with normal tissue, (a) in GSE48418 dataset (b) in GSE30835 dataset (continued) (see online version for colours)

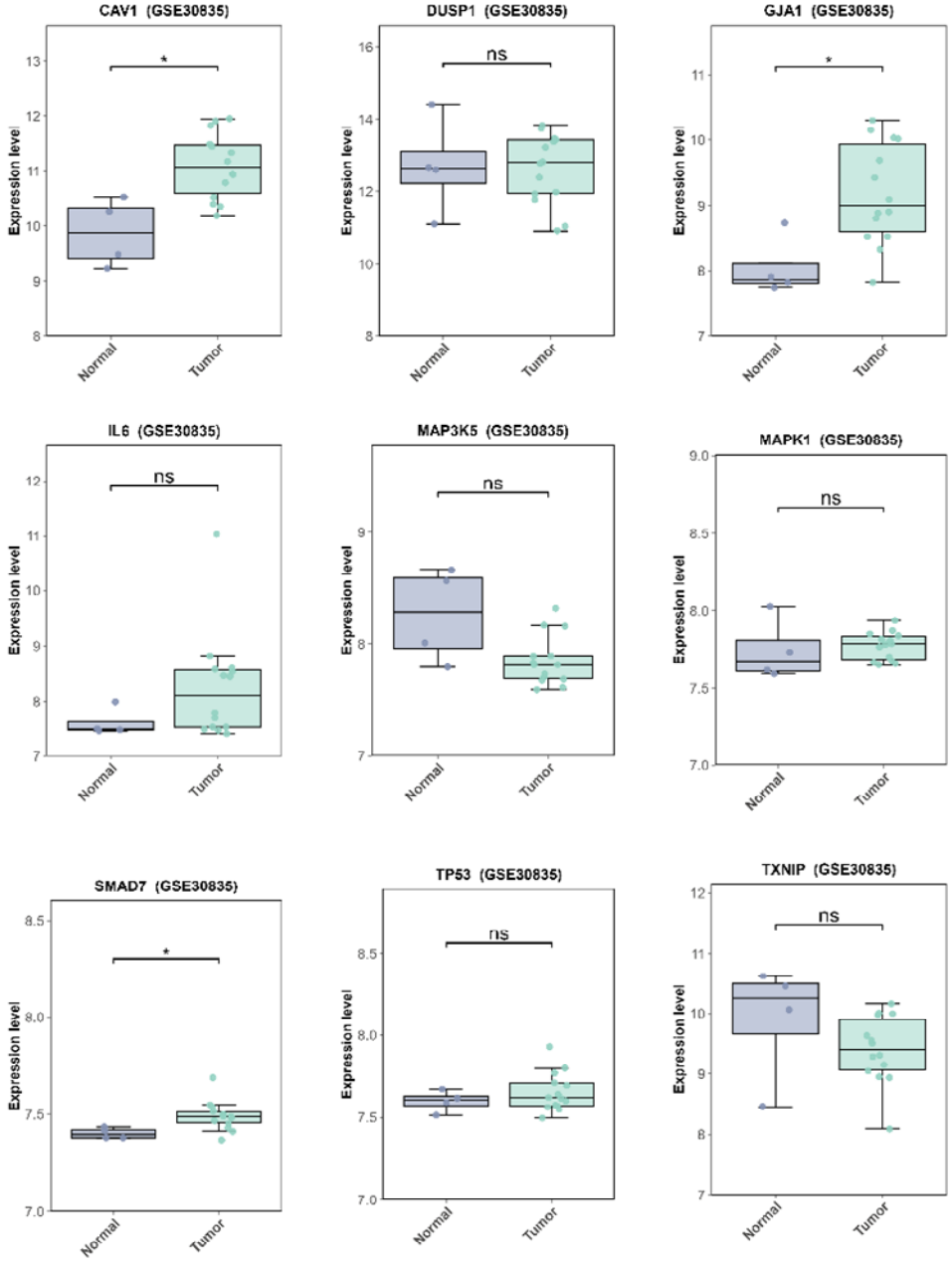

(b)

Note: *$P < 0.05$, **$P < 0.01$, ***$P < 0.001$ and ****$P < 0.0001$.

3.6 Impact of IL6 and GJA1 as core genes on survival of CS patients

After dividing the patients into high and low expression groups based on the median or quartile of the nine identified core genes, the survival analysis was conducted. Core genes with a significance level of $P < 0.05$ were selected as factors associated with the survival of patients. As illustrated in Figure 7, the results demonstrated a significantly higher overall survival rate among patients with high expression of *IL6* ($n = 131$) compared to those with low expression of *IL6* ($n = 131$; $P = 0.008$). Conversely, patients with low expression of *GJA1* (bottom 25%, $n = 66$) exhibited a significantly higher overall survival rate compared to those with high expression of *GJA1* (top 25%, $n = 66$; $P = 0.023$). These data suggested that *IL6* and *GJA1* might use as the prognostic gene for CS patients.

Figure 7 The survival curves for CS patients with different expression level of *IL6* and *GJA1*, (a) the influence of *IL6* expression on the survival curve of CS patients (b) the influence of *GJA1* expression on the survival curve of CS patients (see online version for colours)

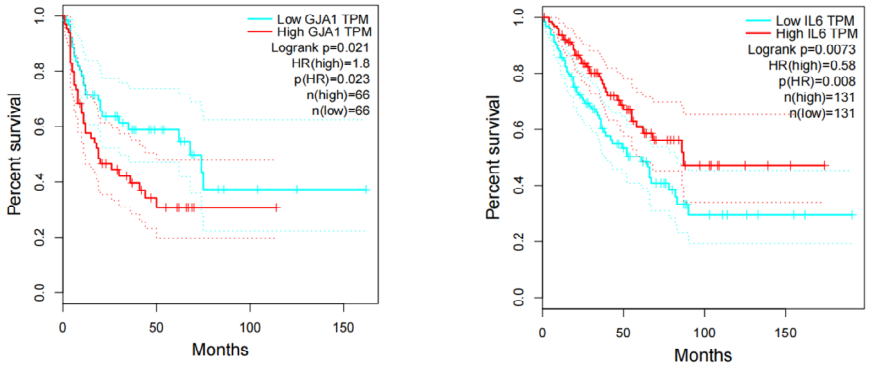

(a) (b)

4 Discussion

CS is the second most common primary bone malignancy mainly influencing adults, and there is obvious trouble in the design of therapeutic plans due to the insensitivity to radiotherapy and chemotherapy (Chow, 2018). Thus, the survival rate of high-grade or clinically metastatic CS patients is poor. The primary objective of this study was to elucidate the molecular mechanisms involved in CS and identify potential core factors associated with the survival rate of CS patients. Through comprehensive bioinformatics analysis, a group of candidate genes including *TP53, GJA1, IL6, CAV1, MAPK1, and SMAD7*, as well as several potential pathways such as TLR signalling pathway, MAPK signalling pathway, and peroxisome pathway were identified. By integrating the protein-protein interaction network and gene-miRNA network, a set of nine intersecting genes (*IL6, TP53, MAPK1, CAV1, GJA1, SMAD7, TXNIP, MAP3K5*, and *DUSP1*) were recognised as crucial genes in the pathogenesis of CS. Notably, among these genes, *GJA1* and *IL6* emerged as promising candidates with the highest likelihood to influence the survival rate of CS patients.

MAPK signalling pathway is the primary regulatory module of various cellular processes such as cell proliferation, differentiation, and stress responses (Sun et al., 2015). It is reported that the MAPK pathway comprises several key signalling components and phosphorylation events that play a role in tumorigenesis. For instance, Li et al. (2024) highlighted that β-eudesmol inhibited cell proliferation and promoted cell apoptosis and ferroptosis via regulating MAPK pathway in breast cancer. Yang et al. (2022) have demonstrated that inhibition of activation of the ROS-ASK1-p38 MAPK signalling pathway promoted the inhibition of proliferation, migration, and invasion of Eca109 and KYSE150 cells and the induction of ferroptosis by realgar. Zhai et al. (2025) have uncovered that Jujuboside B inhibits proliferation and induces apoptosis and ferroptosis in colorectal cancer cells with potential involvement of the MAPK signalling pathway. Besides, peroxisomes are metabolic organelles involved in lipid metabolism and cellular redoxbalance (Kim, 2020). Peroxisomes are major sites of ROS generation and lipid metabolism, both central to ferroptosis, and peroxisome-driven ether-linked phospholipids biosynthesis is essential for ferroptosis (Cui et al., 2021). A previous study has found that *CDH4* inhibits ferroptosis in oral squamous cell carcinoma cells via fatty acid metabolism pathway peroxisome pathway (Xie et al., 2023). In this study, the hub-genes identified from gene-miRNA interaction network were enriched in MAPK signalling pathway and peroxisome pathway. Thus, these data implied that MAPK signalling pathway and peroxisome pathway might exert a significant function in the ferroptosis of CS.

GJA1, also known as gap junction protein alpha 1, is a multifunctional protein that belongs to the gap junction family. It plays a crucial role in mediating intercellular communication and maintaining the fundamental metabolic stability of cells (Meng et al., 2020; Wu et al., 2022b). Numerous studies have reported that dysregulated expression of *GJA1* is associated with cancer progression (Stoletov et al., 2013). Aberrant expression of *GJA1* has been observed in various types of cancer and has been implicated in promoting tumour growth, invasion, and metastasis (Tang et al., 2011; Bišćanin et al., 2016). CS with recurrence and metastasis commonly lead to poor prognosis. Therefore, it is hypothesised that *GJA1* may disrupt intercellular communication in CS cells, leading to alterations in cellular behaviours such as enhanced proliferation, migration, and invasiveness. These changes in cellular behaviour may contribute to the recurrence and metastasis of CS. Zeng et al. (2019) have indicated that *GJA1* may promote the cellular proliferation, migration, and EMT in non-small cell lung cancer via activating p53/MDM2 signalling pathway. Moreover, in this study, *GJA1* was related with both CS and ferroptosis. Ferroptosis is a form of cell death that has attracted significant attention over the past decade. This process is characterised by an accumulation of lipid peroxides within cells, which surpasses the antioxidant capacity of glutathione-dependent peroxidase 4. Consequently, the physical integrity of the plasma membrane is compromised, triggering an osmotic process that leads to cell rupture and ultimately, cell death. In this study, we also found that *GJA1* enriched in GO-BP of cellular response to external stimulus. It's reported that abnormal cellular response to external stimulus, such as excessive proliferation and resistance to apoptosis, can disrupt cellular homeostasis and drive the malignant transformation, invasion and metastasis of cancer cells (Cox and Goding, 1991). Combined with the results of survival analysis, *GJA1* may play vital role in the regulation of ferroptosis in CS, and is tightly associated with the prognosis of patients. Of course, this requires further experiments or other relevant verification.

IL6 is a common inflammatory indicator, and it plays an extremely important role in acute inflammatory response. In this study, we found *IL6* was associated with ferroptosis in CS. In rheumatoid arthritis, ferroptosis has been reported to trigger the innate immunity of the body, promote the release of proinflammatory cytokines such as *IL6*, and promote the uptake of iron by cells (Zhao et al., 2022). Also, Zhou et al. (2022) revealed that *IL6* was a key ferroptosis DEG in lumbosacral spinal root avulsion. A considerable increase in *IL6* levels triggers the production of Hepcidin, a key regulator of iron homeostasis. This action subsequently inhibits Ferroportin (FPN), leading to a rise in intracellular iron and ferritin. This cascade of events provokes the phagocytosis of ferritin, ultimately fostering ferroptosis, also known as iron-induced cell death (Fratta Pasini et al., 2021). It has also been indicated that *IL6* can promote the cellular ferroptosis sensitivity by increasing the levels of the cellular labile iron pool (Dou et al., 2022; Wu et al., 2022a). In this study, we also found that a significantly higher overall survival rate among patients with high expression of *IL6* compared to those with low expression. However, it's reported that *IL6* is typically a pro-tumorigenic and pro-inflammatory cytokine linked to poor prognosis in most cancers (Pennel et al., 2024; Browning et al., 2018). Interestingly, we also found that the expression of *IL6* in CS was significantly lower than that in normal tissue in GSE48418 dataset, while the opposite result was observed in GSE30835 dataset. The reason for this contradictory outcome might be due to the limited sample size and unmatched subtypes. Meanwhile, the activation of TLR is one of the earliest events in the *IL6* generation process, and activation of TLR pathways leads to secretion of *IL6* (Khanmohammadi and Rezaei, 2021). Herein, TLR pathway was involved in the top 15 enriched pathways, and *IL6* enriched in the TLR pathway. Ferrostatin-1 is an inhibitor of ferroptosis, and Wang et al. (2023) have found that ferrostatin-1 inhibits TLR 4/NF-κB signalling to alleviate intervertebral disc degeneration in rats. Lu et al. (2024) have suggested that nicorandil may regulate ferroptosis through TLR4/SLC7A11 signalling, thereby alleviating septic cardiomyopathy. Therefore, it can be speculated that *IL6* may regulate ferroptosis in CS through TLR pathway.

However, all the results were obtained based on the bioinformatics analysis without validated experiment, therefore, the expression and function of the identified nine core genes still need further validation *in in vivo* and *in vitro* experiments. For example, we will conduct western blot and real-time quantitative PCR (qRT-PCR) analysis to confirm the expression of the nine core genes in CS, and knockdown *GJA1* in CS cell lines (SW1353, JJ012) and measure the sensitivity to ferroptosis inducers (e.g., RSL3, Erastin) via lipid peroxidation and cell viability assays. In addition, only one training set and one validation set were used in this study. Due to the limited sample size, only *CAV1* and *GJA1* showed significant differences. Thus, it's necessary to confirm their expression stability in larger sample sizes and in cohorts with matched subtypes in the future. Besides, the ferroptosis-related genes are derived from FerrDb database, which is being updated continuously, and more genes are yet to be discovered. Furthermore, the involved molecular mechanism should be further deeply explored.

5 Conclusions

Our study, through comprehensive bioinformatics analysis, identified key genes and pathways associated with ferroptosis in CS. Nine intersecting genes (*IL6, TP53, MAPK1, CAV1, GJA1, SMAD7, TXNIP, MAP3K5*, and *DUSP1*) played crucial roles in the

pathogenesis of the disease, among which *IL6* and *GJA1* were determined as key factors potentially influencing the survival rate of CS patients. These findings provide vital insights for understanding the pathophysiological mechanism of CS and developing new therapeutic strategies. Although these results require further experimental validation, they set the groundwork for future research and may offer target genes for improving the therapeutic outcomes of CS.

Acknowledgements

Conception and design of the research: Zhiqiang Ye; Acquisition of data: Zhaoyuan Wang; analysis and interpretation of data: Zhiqiang Ye, Zhuo Zhao; statistical analysis: Bowen Zheng; obtaining funding: Haidong Liang; drafting the manuscript: Jinghang Lu, Lianbo Yang; revision of manuscript for important intellectual content: Yongxu Zhang.

Funding

This study was supported by Effects of Mulberry, Poria Cocos and Lycium Barbarum on Bone Growth and Metabolism in Simulated Weight – less Rats (No. 21Z12006) and Research on the Application of HoloLens in Microsurgery Teaching (No. 2022JXGGYJ006).

Data availability

The datasets generated and analysed during the current study are available from the corresponding author on reasonable request.

Declarations

All authors declare that they have no conflicts of interest.

References

Bišćanin, A., Ljubičić, N., Boban, M., Baličević, D., Pavić, I., Bišćanin, M.M., Budimir, I., Dorosulic, Z. and Duvnjak, M. (2016) 'CX43 expression in colonic adenomas and surrounding mucosa is a marker of malignant potential', *Anticancer Res*., Vol. 36, No. 9, pp.5437–5442.

Browning, L., Patel, M.R., Horvath, E.B., Tawara, K. and Jorcyk, C.L. (2018) 'IL-6 and ovarian cancer: inflammatory cytokines in promotion of metastasis', *Cancer Manag. Res.*, Vol. 10, No. 1, pp.6685–6693.

Chen, C., Zhou, H., Xu, L., Liu, X., Liu, Z., Ma, D., Chen, Y. and Ma, Q. (2010) 'Prognostic significance of downregulated expression of programmed cell death 5 in chondrosarcoma', *J. Surg. Oncol*,. Vol. 102, No. 7, pp.838–843.

Chen, H. and Boutros, P.C. (2011) 'VennDiagram: a package for the generation of highly-customizable Venn and Euler diagrams in R', *BMC Bioinformatics*, Vol. 12, No. 1, p.35.

Chen, X., Kang, R., Kroemer, G. and Tang, D. (2021) 'Broadening horizons: the role of ferroptosis in cancer', *Nat. Rev. Clin. Oncol.*, Vol. 18, No. 5, pp.280–296.

Chow, W.A. (2018) 'Chondrosarcoma: biology, genetics, and epigenetics', *F1000Res*, Vol. 7, No. 5, p.1826.

Cox, P.M. and Goding, C.R. (1991) 'Transcription and cancer', *Br. J. Cancer*, Vol. 63, No. 5, pp.651–662.

Cui, W., Liu, D., Gu, W. and Chu, B. (2021) 'Peroxisome-driven ether-linked phospholipids biosynthesis is essential for ferroptosis', *Cell Death Differ*., Vol. 28, No. 8, pp.2536–2551.

Dou, J., Liu, X., Yang, L., Huang, D. and Tan, X. (2022) 'Ferroptosis interaction with inflammatory microenvironments: mechanism, biology, and treatment', *Biomed Pharmacother*, November, Vol. 155, Article 113711.

Fratta Pasini, A.M., Stranieri, C., Girelli, D., Busti, F. and Cominacini, L. (2021) 'Is ferroptosis a key component of the process leading to multiorgan damage in COVID-19?', *Antioxidants (Basel)*, Vol. 10, No. 11, p.1677.

Jiang, M., Jike, Y., Liu, K., Gan, F., Zhang, K., Xie, M., Zhang, J., Chen, C., Zou, X., Jiang, X., Dai, Y., Chen, W., Qiu, Y. and Bo, Z. (2023) 'Exosome-mediated miR-144-3p promotes ferroptosis to inhibit osteosarcoma proliferation, migration, and invasion through regulating ZEB1', *Mol. Cancer*, Vol. 22, No. 1, p.113.

Khanmohammadi, S. and Rezaei, N. (2021) 'Role of toll-like receptors in the pathogenesis of COVID-19.', *J. Med. Virol.*, Vol. 93, No. 5, pp.2735–2739.

Kim, J.A. (2020) 'Peroxisome metabolism in cancer', *Cells*, Vol. 9, No. 7, p.1692.

Li, Z., Li, J., Liu, X., Liu, Y., Chen, H. and Sun, X. (2024) 'β-eudesmol inhibits cell proliferation and induces ferroptosis via regulating MAPK signaling pathway in breast cancer', *Toxicon*., Vol. 237, p.107529.

Liu, Q. and Wang, K. (2019) 'The induction of ferroptosis by impairing STAT3/Nrf2/GPx4 signaling enhances the sensitivity of osteosarcoma cells to cisplatin', *Cell Biol. Int*., Vol. 43, No. 11, pp.1245–1256.

Liu, X., Du, S., Wang, S. and Ye, K. (2022) 'Ferroptosis in osteosarcoma: a promising future', *Front Oncol*., Vol. 12, p.1031779.

Liu, Z. and Liu, X. (2025) 'Prognostic model of osteosarcoma based on telomere-related genes and analysis of immune characteristics', *Int. Immunopharmacol*, Vol. 151, p.114198.

Lu, J.S., Wang, J.H., Han, K. and Li, N. (2024) 'Nicorandil regulates ferroptosis and mitigates septic cardiomyopathy via TLR4/SLC7A11 signaling pathway', *Inflammation*, Vol. 47, No. 3, pp.975–988.

Luo, Y., Gao, X., Zou, L., Lei, M., Feng, J. and Hu, Z. (2021) 'Bavachin induces ferroptosis through the STAT3/P53/SLC7A11 axis in osteosarcoma cells', *Oxid. Med. Cell. Longev.*, Vol. 2021, p.1783485.

Ma, Y., Cong, L., Shen, W., Yang, C. and Ye, K. (2024) 'Ferroptosis defense mechanisms: the future and hope for treating osteosarcoma', *Cell Biochem Funct*., Vol. 42, No. 4, p.e4080.

Meng, S., Fan, X., Zhang, J., An, R. and Li, S. (2020) 'GJA1 expression and its prognostic value in cervical cancer', *Biomed Res Int*., Vol. 2020, p.8827920.

Miwa, S., Yamamoto, N., Hayashi, K., Takeuchi, A., Igarashi, K. and Tsuchiya, H. (2022) 'Therapeutic targets and emerging treatments in advanced chondrosarcoma', *Int. J. Mol. Sci*., Vol. 23, No. 3.

Pennel, K.A.F., Kurniawan, A., Samir Foad Al-Badran, S., Schubert Santana, L., Quinn, J., Nixon, C., Hatthakarnkul, P., Maka, N., Roxburgh, C., Mcmillan, D. and Edwards, J. (2024) 'IL6 and IL6R as prognostic biomarkers in colorectal cancer', *Biomolecules*, Vol. 14, No. 12.

Pennington, Z., Ehresman, J., Pittman, P.D., Ahmed, A.K., Lubelski, D., Mccarthy, E.F., Goodwin, C.R. and Sciubba, D.M. (2021) 'Chondrosarcoma of the spine: a narrative review', *Spine J.*, Vol. 21, pp.2078–2096.

Qiu, C., Liu, T., Luo, D., Luan, D., Cheng, L. and Wang, S. (2022) 'Novel therapeutic savior for osteosarcoma: the endorsement of ferroptosis', *Front. Oncol.*, Vol. 12, p.746030.

Ritchie, M.E., Phipson, B., Wu, D., Hu, Y., Law, C.W., Shi, W. and Smyth, G.K. (2015) 'Limma powers differential expression analyses for RNA-sequencing and microarray studies', *Nucleic Acids Res.*, Vol. 43, No. 12, p.e47.

Song, C., Wang, L., Zhang, F., Lv, C., Meng, M., Wang, W. and Zhou, W. (2024) 'DUSP6 protein action and related hub genes prevention of sepsis-induced lung injury were screened by WGCNA and Venn', *Int. J. Biol. Macromol.*, Vol. 279, No. 1, p.135117.

Stockwell, B.R., Friedmann Angeli, J.P., Bayir, H., Bush, A.I., Conrad, M., Dixon, S.J., Fulda, S., Gascon, S., Hatzios, S.K., Kagan, V.E., Noel, K., Jiang, X., Linkermann, A., Murphy, M.E., Overholtzer, M., Oyagi, A., Pagnussat, G.C., Park, J., Ran, Q., Rosenfeld, C.S., Salnikow, K., Tang, D., Torti, F.M., Torti, S.V., Toyokuni, S., Woerpel, K.A. and Zhang, D.D. (2017) 'Ferroptosis: a regulated cell death nexus linking metabolism, redox biology, and disease', *Cell*, Vol. 171, No. 2, pp.273–285.

Stockwell, B.R., Jiang, X. and Gu, W. (2020) 'Emerging mechanisms and disease relevance of ferroptosis', *Trends Cell Biol.*, Vol. 30, No. 6, pp.478–490.

Stoletov, K., Strnadel, J., Zardouzian, E., Momiyama, M., Park, F.D., Kelber, J.A., Pizzo, D.P., Hoffman, R., Vandenberg, S.R. and Klemke, R.L. (2013) 'Role of connexins in metastatic breast cancer and melanoma brain colonization', *J. Cell Sci.*, Vol. 126, No. 4, pp.904–913.

Sun, Y., Liu, W.Z., Liu, T., Feng, X., Yang, N. and Zhou, H.F. (2015) 'Signaling pathway of MAPK/ERK in cell proliferation, differentiation, migration, senescence and apoptosis', *J. Recept. Signal Transduct. Res.*, Vol. 35, No. 6, pp.600–604.

Szklarczyk, D., Gable, A.L., Nastou, K.C., Lyon, D., Kirsch, R., Pyysalo, S., Doncheva, N.T., Legeay, M., Fang, T., Bork, P., Jensen, L.J. and Von Mering, C. (2021) 'The STRING database in 2021: customizable protein-protein networks, and functional characterization of user-uploaded gene/measurement sets', *Nucleic Acids Res.*, Vol. 49, No. 1, pp.D605–D612.

Tang, B., Peng, Z.H., Yu, P.W., Yu, G. and Qian, F. (2011) 'Expression and significance of Cx43 and E-cadherin in gastric cancer and metastatic lymph nodes', *Med. Oncol.*, Vol. 28, No. 2, pp.502–508.

Thorkildsen, J., Norum, O.J., Myklebust, T.A. and Zaikova, O. (2021) 'Chondrosarcoma local recurrence in the cancer registry of Norway cohort (1990-2013): patterns and impact', *J. Surg. Oncol.*, Vol. 123, No. 2, pp.510–520.

Wang, Y.G., Yu, X.J., Qu, Y.K., Lu, R., Li, M.W., Xu, H.R., Wang, S.X., Guo, X.Z., Kang, H., You, H. and Xu, Y. (2023) 'Ferrostatin-1 inhibits toll-like receptor 4/NF-κB signaling to alleviate intervertebral disc degeneration in rats', *Am. J. Pathol.*, Vol. 193, No. 4, pp.430–441.

Weinschenk, R.C., Wang, W.L. and Lewis, V.O. (2021) 'Chondrosarcoma', *J. Am. Acad. Orthop. Surg.*, Vol. 29, No. 13, pp.553–562.

Wu, J., Feng, Z., Chen, L., Li, Y., Bian, H., Geng, J., Zheng, Z.H., Fu, X., Pei, Z., Qin, Y., Yang, L., Zhao, Y., Wang, K., Chen, R., He, Q., Nan, G., Jiang, X., Chen, Z.N. and Zhu, P. (2022a) 'TNF antagonist sensitizes synovial fibroblasts to ferroptotic cell death in collagen-induced arthritis mouse models', *Nat. Commun.*, Vol. 13, p.676.

Wu, L., Wang, Z., He, X., Jiang, Y., Pan, R., Chen, S., Chen, Y., Han, Y., Yu, H. and Zhang, T. (2022b) 'GJA1 reverses arsenic-induced EMT via modulating MAPK/ERK signaling pathway', *Toxicol Appl. Pharmacol.*, Vol. 450, p.116138.

Xie, J., Lan, T., Zheng, D.L., Ding, L.C. and Lu, Y.G. (2023) 'CDH4 inhibits ferroptosis in oral squamous cell carcinoma cells', *BMC Oral Health*, Vol. 23, No. 1, p.329.

Yang, R., Chen, F., Xu, H., Guo, Z., Cao, C., Zhang, H. and Zhang, C. (2022) 'Exploring the mechanism of realgar against esophageal cancer based on ferroptosis induced by ROS-ASK1-p38 MAPK signaling pathway', *Evid. Based Complement Alternat. Med.*, Vol. 2022, p.3698772.

Yu, G., Wang, L.G., Han, Y. and He, Q.Y. (2012) 'clusterProfiler: an R package for comparing biological themes among gene clusters', *Omics*, Vol. 16, No. 5, pp.284–287.

Zeng, S.G., Lin, X., Liu, J.C. and Zhou, J. (2019) 'Hypoxia-induced internalization of connexin 26 and connexin 43 in pulmonary epithelial cells is involved in the occurrence of non-small cell lung cancer via the P53/MDM2 signaling pathway', *Int. J. Oncol.*, Vol. 55, No. 4, pp.845–859.

Zhai, K., Liu, G., Cao, C. and Wang, X. (2025) 'Jujuboside B inhibits proliferation and induces apoptosis and ferroptosis in colorectal cancer cells with potential involvement of the MAPK signaling pathway', *Oncol. Lett.*, Vol. 29, No. 3, p.162.

Zhao, T., Yang, Q., Xi, Y., Xie, Z., Shen, J., Li, Z., Li, Z. and Qin, D. (2022) 'Ferroptosis in rheumatoid arthritis: a potential therapeutic strategy', *Front. Immunol.*, Vol. 13, p.779585.

Zhou, Z., Lu, J., Ma, J. and Zhu, L. (2022) 'Identification of potential ferroptosis key genes in the pathogenesis of lumbosacral spinal root avulsion by RNA sequencing and bioinformatics analysis', *Front Mol. Biosci.*, Vol. 9, p.902607.

Supplementary

Table S1 The list of 70 intersection genes associated with ferroptosis in CS

Gene name	*Gene name*	*Gene name*	*Gene name*
RGS4	LCN2	SAT1	CAPG
IDH2	DECR1	FTH1	ATG7
KLF2	PARP12	DUSP1	KIF20A
MT1G	CEBPG	PARP16	PEBP1
BEX1	PRDX6	AKR1C3	IL1B
ALB	PDK4	NNMT	RPL8
CAV1	ACO1	HMOX1	FURIN
PHF21A	OSBPL9	MAPK1	ADAM23
PARP9	SLC38A1	PARP4	CTSB
BRD3	SREBF1	SLC1A4	SLC7A5
AURKA	GJA1	GPT2	PEX6
GSTM1	BRD7	PAQR3	SCD
TFAP2A	MYCN	ANO6	HMGB1
P53	ETV4	ACSL1	MAP3K5
PARP14	SLC40A1	TMBIM4	GDF15
IL6	LAMP2	GALNT14	TXNIP
NDRG1	AIFM2	SLC2A6	SMAD7
DDIT4	JUN		

Table S2 Enrichment analysis of the core genes

ID	*Gene*
hsa05020	IL6
hsa04620	IL6
hsa05142	IL6
hsa04621	IL6
hsa05332	IL6
hsa05144	IL6
hsa04623	IL6
GO:0006979	IL6
GO:0062197	IL6
GO:0034599	IL6
GO:0000302	IL6
GO:0042542	IL6
GO:0034614	IL6
hsa04010	TP53
hsa05210	TP53
hsa04722	TP53
hsa05216	TP53
hsa05219	TP53
hsa05213	TP53
hsa05014	TP53
hsa05223	TP53
GO:0071496	TP53
GO:0031669	TP53
GO:0031668	TP53
GO:0009267	TP53
GO:0006979	TP53
GO:0031667	TP53
GO:0042594	TP53
GO:0062197	TP53
GO:0034599	TP53
GO:0062012	TP53
GO:1901216	TP53
GO:0072593	TP53
hsa05020	MAPK1
hsa04620	MAPK1
hsa05142	MAPK1
hsa04010	MAPK1
hsa04621	MAPK1

Table S2 Enrichment analysis of the core genes (continued)

ID	*Gene*
hsa05210	MAPK1
hsa04722	MAPK1
hsa05140	MAPK1
hsa05216	MAPK1
hsa05219	MAPK1
hsa04150	MAPK1
hsa05213	MAPK1
hsa05223	MAPK1
GO:0071496	MAPK1
GO:0031669	MAPK1
GO:0031668	MAPK1
GO:0009267	MAPK1
GO:0006979	MAPK1
GO:0031667	MAPK1
GO:0042594	MAPK1
GO:0062197	MAPK1
GO:0034599	MAPK1
GO:0000302	MAPK1
GO:0010038	MAPK1
GO:0071276	MAPK1
GO:0034614	MAPK1
GO:0046686	MAPK1
GO:0062197	CAV1
GO:0010038	CAV1
GO:0062012	CAV1
GO:0120162	CAV1
GO:0001659	CAV1
GO:0033137	CAV1
GO:0071496	GJA1
GO:0120162	GJA1
GO:0001659	GJA1
GO:0033137	SMAD7
GO:0006979	TXNIP
GO:0000302	TXNIP
GO:0010038	TXNIP
GO:0042542	TXNIP
hsa04010	MAP3K5
hsa04722	MAP3K5

Table S2 Enrichment analysis of the core genes (continued)

ID	*Gene*
hsa05014	MAP3K5
GO:0071496	MAP3K5
GO:0031669	MAP3K5
GO:0031668	MAP3K5
GO:0009267	MAP3K5
GO:0006979	MAP3K5
GO:0031667	MAP3K5
GO:0042594	MAP3K5
GO:0062197	MAP3K5
GO:0034599	MAP3K5
GO:0000302	MAP3K5
GO:0042542	MAP3K5
GO:1901216	MAP3K5
GO:0034614	MAP3K5
hsa04010	DUSP1
GO:0006979	DUSP1
GO:0000302	DUSP1
GO:0010038	DUSP1
GO:0042542	DUSP1